Insight into the in-cloud formation of oxalate based on in-situ measurement by single particle mass spectrometry

Guohua Zhang[1], Qinhao Lin[1,2], Long Peng[1,2], Yuxiang Yang[1,2], Yuzhen Fu[1,2], Xinhui Bi[1,*], Mei Li[3], Duohong Chen[4], Jianxin Chen[5], Zhang Cai[6], Xinming Wang[1], Ping'an Peng[1], Guoying Sheng[1], Zhen Zhou[3]

[1] State Key Laboratory of Organic Geochemistry and Guangdong Key Laboratory of Environmental Resources Utilization and Protection, Guangzhou Institute of Geochemistry, Chinese Academy of Sciences, Guangzhou 510640, PR China

[2] University of Chinese Academy of Sciences, Beijing 100039, PR China

[3] Atmospheric Environment Institute of Safety and Pollution Control, Jinan University, Guangzhou 510632, PR China

[4] State Environmental Protection Key Laboratory of Regional Air Quality Monitoring, Guangdong Environmental Monitoring Center, Guangzhou 510308, PR China

[5] Shaoguan Environmental Monitoring Center, Shaoguan 512026, PR China

[6] John and Willie Leone Family Department of Energy and Mineral Engineering, The Pennsylvania State University, University Park, PA 16802, USA

Instrumentation

SPAMS

Individual particles are introduced into SPAMS through a critical orifice. They are focused and accelerated to specific velocities, which are determined by two continuous diode Nd:YAG laser beams (532 nm). Based on the measured velocities, a pulsed laser (266 nm) downstream is trigger to desorp/ionize the particles. The produced positive and negative molecular fragments are recorded. In summary, a velocity, a detection moment, and an ion mass spectrum are recorded for each ionized particle, while there is no mass spectrum for not ionized particles. The velocity could be converted to d_{va} based on a calibration using polystyrene latex spheres (PSL, Duke Scientific Corp., Palo Alto) with predefined sizes.

Table S1. Correlation analysis between the hourly detected number for species in cloud-free particles (N = 109) and ***cloud RES*** particles (N = 123). Most of the analysis shows significant correlation ($p < 0.001$) between the species, with the R^2 shown as follows. Results without significant correlation are marked with superscripts a and b.

	m/z -45	**m/z -59**	**m/z -71**	**m/z -73**	**m/z -89**	**K.rich**
m/z -45	1					
m/z -59	0.92/***0.93***	1				
m/z -71	0.77/***0.33***	0.92/***0.35***	1			
m/z -73	0.94/***0.81***	0.92/***0.86***	0.80/***0.20***	1		
m/z -89	0.22/***0.32***	0.38/***0.45***	0.46/***0.12***	0.33/***0.64***	1	
K.rich	0.52/**0.58**	0.33/**0.59**	0.21/***0*** [a]	0.57/***0.72***	0.05 [b] /**0.41**	1

[a] $p = 0.37$; [b] $p = 0.009$.

Table S2. Number fraction (%) of ion peaks for organic acids associated with all the detected particles and K-rich particles, respectively.

Ion peaks	All the detected particles (%)	K-rich particles (%)
m/z -45	12.4 ± 0.1	21.5 ± 0.3
m/z -59	8.6 ± 0.1	16.5 ± 0.3
m/z -71	2.8 ± 0.1	5.6 ± 0.1
m/z -73	12.6 ± 0.1	22.5 ± 0.3

Table S3. Number fraction (%) of the major OAs relative to all the detected particles during each cloud event.

Ion peaks	Cloud I	Cloud II	Cloud III
m/z -45	16.5 ± 11.1	4.8 ± 1.2	8.6 ± 4.7
m/z -59	16.0 ± 9.6	3.9 ± 1.2	8.6 ± 5.5
m/z -71	8.7 ± 7.3	0.6 ± 0.4	4.0 ± 4.1

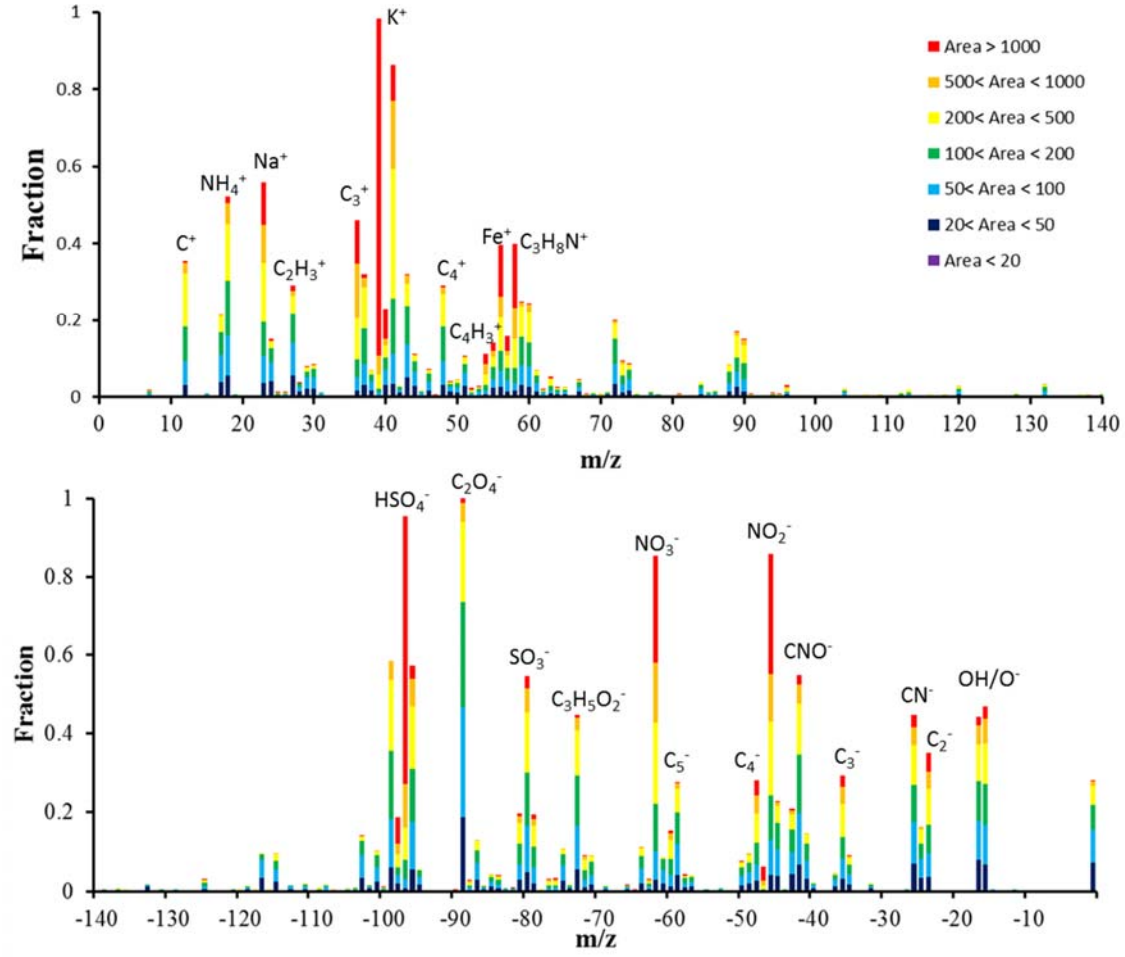

Figure S1. The number-based digitized mass spectrum of all the detected oxalate-containing particles.

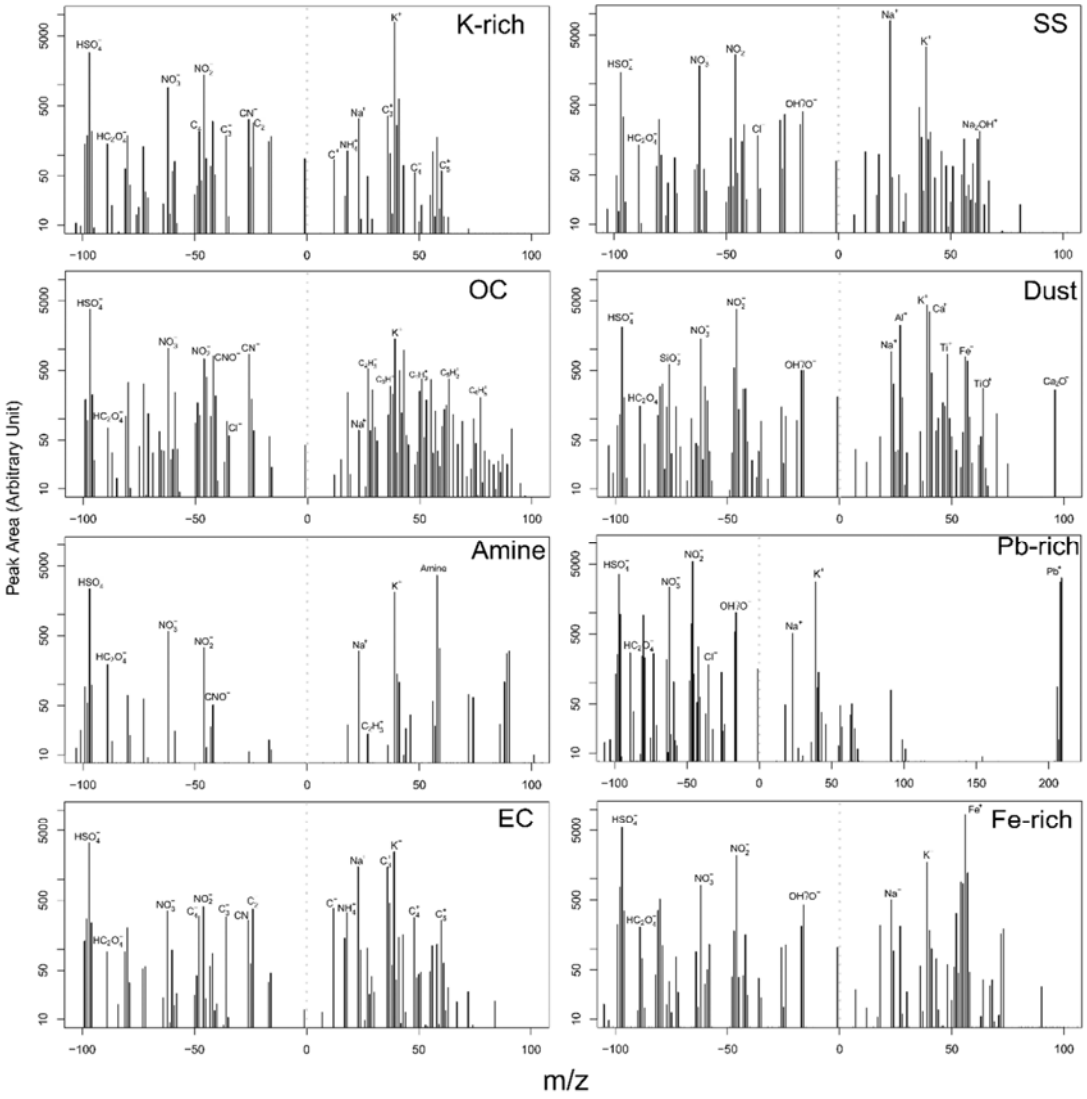

Figure S2. Average mass spectra for each particle type of oxalate-containing particles. Representative ions peaks were labeled for each particle types.

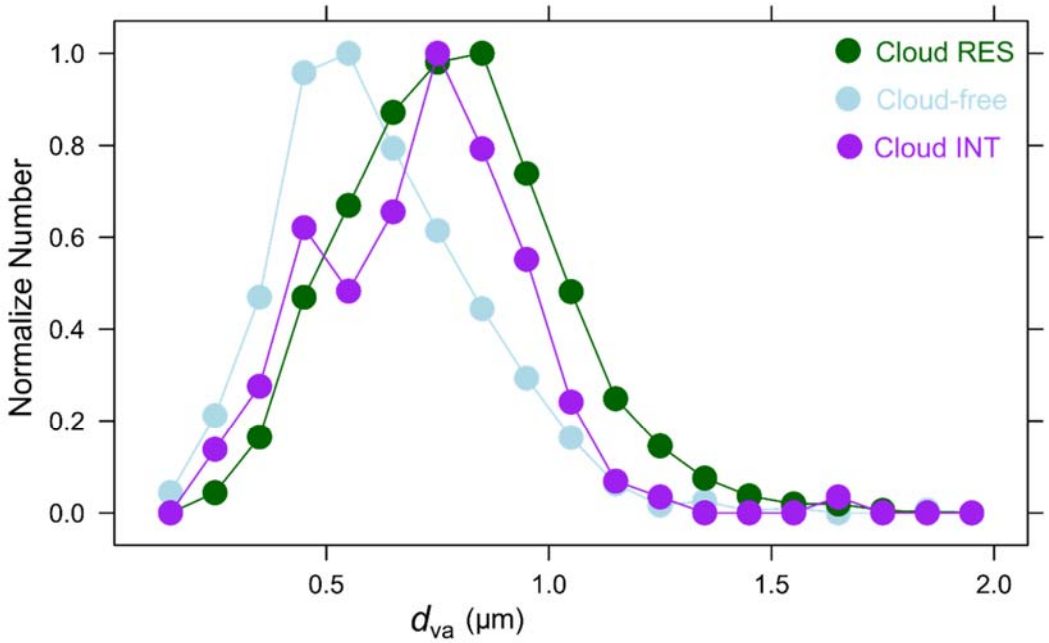

52

53 Figure S3. The normalized unscaled number size distribution of oxalate-containing

54 particles in cloud-free, RES, and INT particles, respectively.

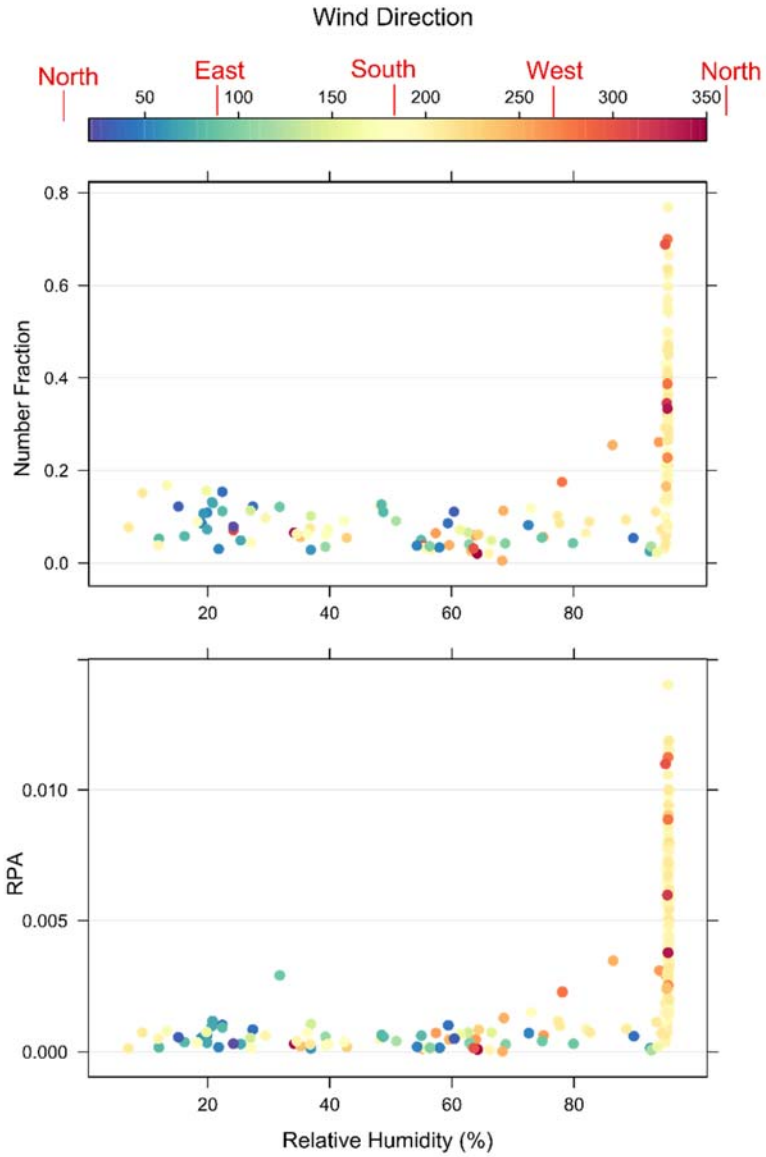

55
56

57 Figure S4. Scattering plots of (a) the number fraction and (b) the RPA of the oxalate-

58 containing particles versus relative humidity. The coloration indicates the wind direction.

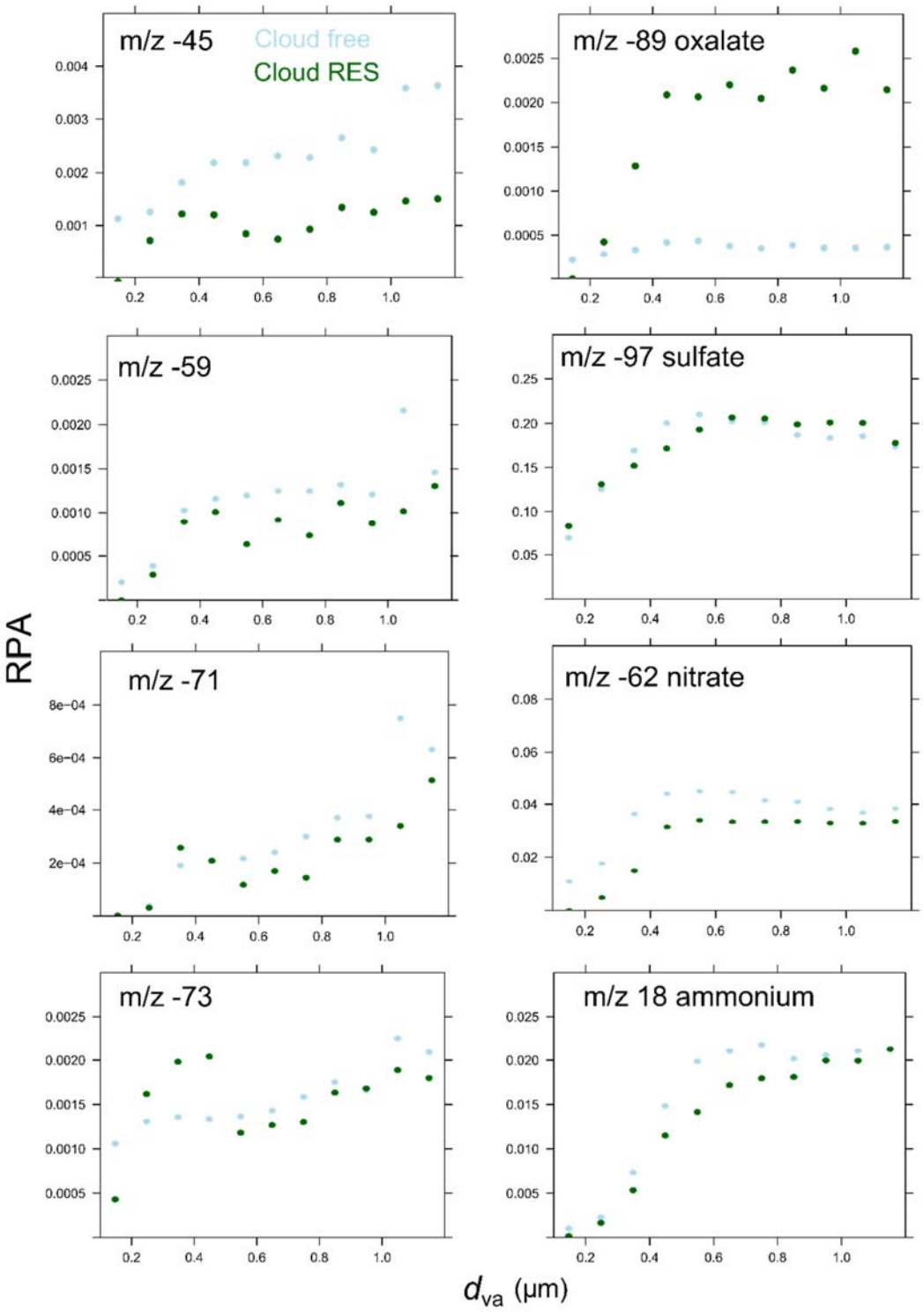

Figure S5. Size-resolved distribution of RPAs for each species in the cloud-free and RES particles.

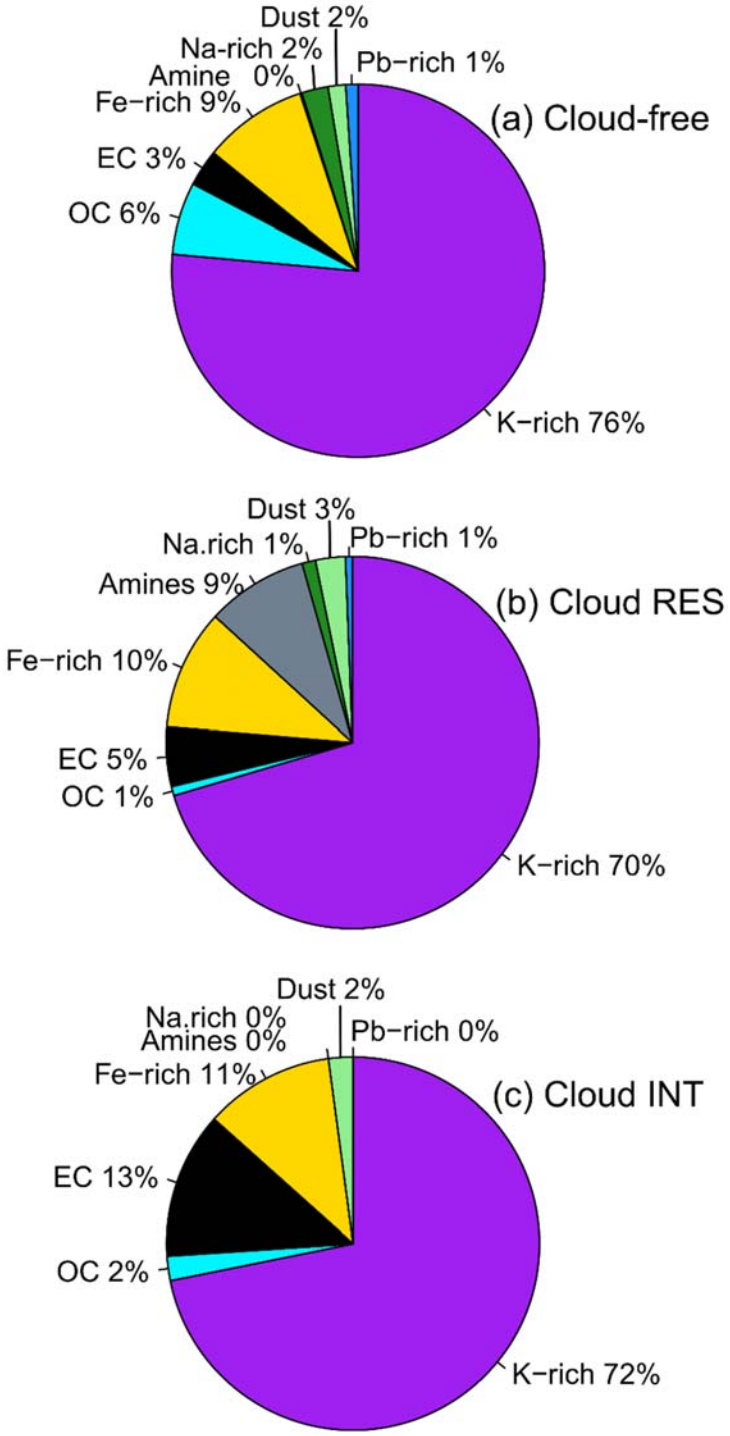

62

63 Figure S6. Number fraction of each oxalate-containing particle type for the (a) cloud-free,

64 (b) RES, and (c) INT particles, respectively.

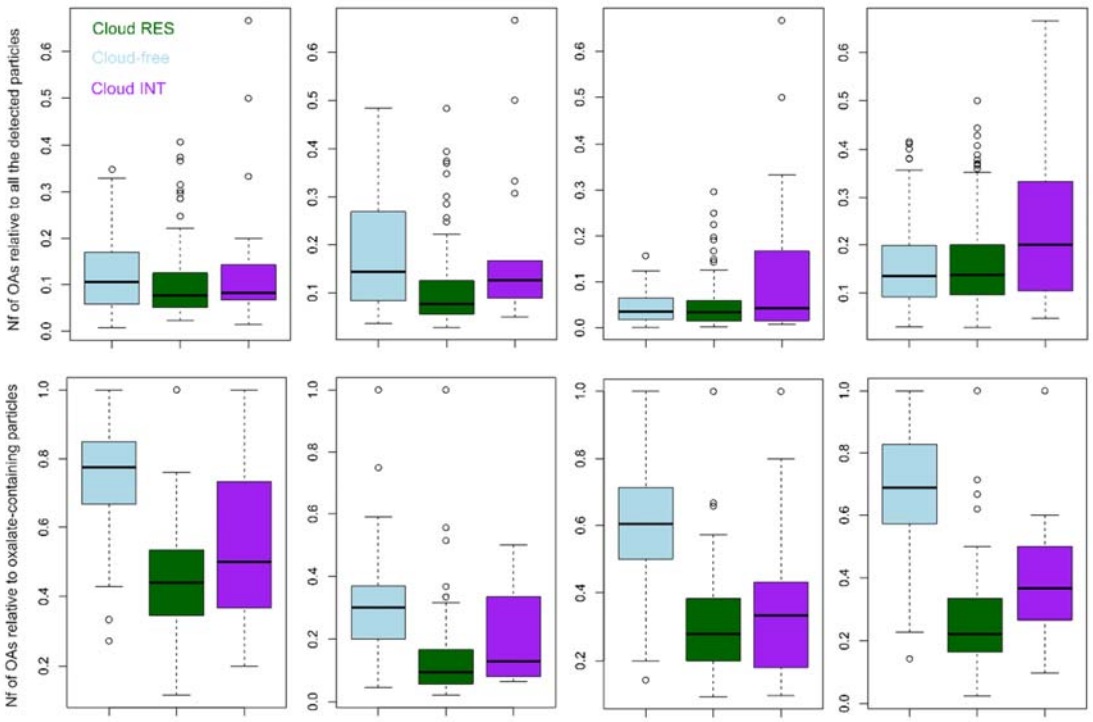

Figure S7. Box and whisker plot of the variations of number fractions for four OAs in (a-d) all the detected particles, and (e-h) oxalate-containing particles, separated for cloud-free, RES, and INT particles, respectively. In a box and whisker plot, the lower, median and upper line of the box denote the 25, 50, and 75 percentiles, respectively; the lower and upper edges of the whisker denote the 10 and 90 percentiles, respectively.